

Electron temperature fluctuations in 30 Doradus

A. C. Krabbe¹ and M. V. F. Copetti^{1,2}

¹ Laboratório de Análise Numérica e Astrofísica, Departamento de Matemática,
Universidade Federal de Santa Maria, 97119-900 Santa Maria, RS, Brazil

² Physics Department, University of Cincinnati, Cincinnati OH 45221-0011, USA

Received 13 December 2001 / Accepted 18 February 2002

Abstract. We present an observational study of the spatial variation of the electron temperature in the 30 Doradus Nebula. We used the $[\text{O III}](\lambda 4959 + \lambda 5007)/\lambda 4363$ ratio to estimate the electron temperature at 135 positions in the nebula across three different directions. We analysed long-slit spectrophotometric data of high signal-to-noise in the range of 4100 to 5030 Å obtained with the Cassegrain spectrograph attached to the 1.60 m telescope of the Laboratório Nacional de Astrofísica, Brazil. No large-scale electron temperature gradient was detected in 30 Doradus. The electron temperature estimates obtained are fairly homogeneous with a mean value of 10270 ± 140 (3σ) K. The compatibility between the present estimates with optical and radio temperature determinations found in the literature for other positions or for the entire nebula corroborates this conclusion. Temperature fluctuations of small amplitude were observed with a variance relative to the mean of $t_s^2 = 0.0025$ or equivalently with a dispersion of only 5%. The areas with lower surface brightness seem to present slightly higher electron temperatures. This would indicate that the bright arcs of 30 Doradus, which correspond to the densest regions, would have lower electron temperatures than the most diffuse areas.

Key words. ISM: H II regions – ISM: individual objects: 30 Doradus Nebula

1. Introduction

Traditionally, the abundances in planetary nebulae and H II regions of chemical elements other than hydrogen and helium have been obtained from their collisionally excited emission lines. Since the emissivities of these lines are exponentially dependent on the electron temperature, T_e , an accurate determination of this property is a key step in this process. However, considerable differences are found between the temperature estimates based on distinct methods. These discrepancies have been attributed to internal spatial temperature fluctuations in the nebulae (Peimbert 1967).

The recent developments in astronomical instruments have made possible the determination of the abundances of CNO elements based on their recombination lines. These lines are 10^3 – 10^4 times fainter than the strong forbidden lines. So, the use of this method is limited to a few objects with very high surface brightness. On the other hand, it has the advantage of being only weakly dependent on the electron temperature. Huge discrepancies between abundance determinations from collisionally excited and recombination lines have been reported in the

literature, which cast doubt on the accuracy of the abundance determinations in gaseous nebulae. For example, Liu et al. (1995) determined abundances of C, N and O in the planetary nebula NGC 7009 by recombination lines and found that they are about 5 times higher than those derived from forbidden lines. These discrepancies have also been explained by the presence of fluctuations of electron temperature. However, the magnitudes of the temperature fluctuations needed are considerably higher than those predicted by standard photoionisation models and the physical mechanisms that could possibly explain the large temperature fluctuations presumed are unknown. So, the subject of spatial variations of electron temperature in H II regions and planetary nebulae has gained renewed interest.

In the present paper, we report the results of a study on the spatial variation of the electron temperature in the 30 Doradus Nebula based on point-to-point measurements of the $[\text{O III}](\lambda 4959 + \lambda 5007)/\lambda 4363$ line ratio obtained from long-slit spectrophotometric observations of high signal-to-noise ratio.

2. Observations and data reduction

The observations were performed during the nights of September 12/13 1994 and April 14/15 2001 at the Laboratório Nacional de Astrofísica (LNA), Brazil, with

Send offprint requests to: M. V. F. Copetti,
e-mail: angela,mvfc@lana.ccne.ufsm.br

Table 1. Journal of observations.

Date	Exp. time (s)	$\alpha(2000)$	$\delta(2000)$	PA
9.12.1994	3×1200	5 ^h 38 ^m 42 ^s .4	−69°06′01″	26°
9.12.1994	2×1200+600	5 ^h 38 ^m 38 ^s .2	−69°05′42″	58°
4.14.2001	3×1200	5 ^h 38 ^m 41 ^s .5	−69°05′14″	90°

the Cassegrain spectrograph attached to the 1.6 m telescope. An EEV CCD of 800×1024 pixels and a SITe CCD of 1024×1024 pixels were used in 1994 and 2001, respectively. A grid of 1200 grooves mm^{-1} was used. The spatial scale was $0.90'' \text{pxl}^{-1}$ for the EEV CCD and $1.0'' \text{pxl}^{-1}$ for the SITe CCD. The slit used had an entrance of $2.5'' \times 360''$ on the plane of the sky. The spectra obtained covered the wavelength range of 4100 to 5030 Å with a dispersion of 0.87 Å pxl^{-1} and a resolution of 2.8 Å, measured as the full-width-at-half-maximum (FWHM) of the emission lines of comparison lamps. Exposures of dome flat-fields and several measurements of bias were made during each night. For flux calibration, the spectrophotometric standard stars LTT 7379, EG 274, HR 9087 and HR 1544 were observed during the 1994 run and HR 3454 and HR 4963 during the 2001 run. Spectra of a He-Ar-Ne lamp were taken before and after each object exposure for wavelength calibration.

Nine two-dimensional spectra of the 30 Doradus Nebula were obtained at three different slit positions. The exposure times were limited to 1200 s. to minimize the effects of cosmic rays and to avoid saturation of the brightest emission lines. Table 1 lists the number and time of the exposures, the equatorial coordinates of the slit center and its position angle, PA, measured from north through east.

The data reduction was made using the *IRAF* software. We have followed the standard procedures for bias correction, flat-fielding, cosmic ray cleaning and wavelength and flux calibrations. In order to increase the signal-to-noise ratio, a rebinning of 5 (EEV) and 4.5 (SITe) CCD rows along the spatial direction was performed, leading to a final spatial scale of $4.5'' \text{pxl}^{-1}$. The two-dimensional spectra were divided into series of one-dimensional spectra, each one corresponding to an aperture of $2.5'' \times 4.5''$.

The line intensities were measured by integrating the flux over a linear local continuum between two given limits. These measurements were made with the *splot* routine of the *IRAF* package. All the line intensities were normalized to $\text{H}\beta$. The error estimates were calculated by $\sigma^2 = \sigma_{\text{cont}}^2 + \sigma_{\text{line}}^2$, where σ_{cont} and σ_{line} are the continuum rms and the Poisson error of the line respectively. The effect of interstellar extinction was corrected by comparing the $\text{H}\gamma/\text{H}\beta$ ratios measured in each aperture with the theoretical ones by Hummer & Storey (1987) for an electron temperature of 10 000 K and a density of 100 cm^{-3} . The reddening law of Howarth (1983) appropriate for the Large Magellanic Cloud was used.

3. Determination of the electron temperature

The electron temperatures were calculated from the $[\text{O III}](\lambda 4959 + \lambda 5007)/\lambda 4363$ intensity ratios by resolving numerically the equations of equilibrium for the five-level atom using the *temden* routine of the *nebular* package of *IRAF*. The values of energy levels, transition probabilities and collision strengths used were from Bowen (1960), Wiese et al. (1996) and Lennon & Burke (1994) respectively. In this method there is a dependence of electron temperature T_e on the electron density N_e assumed. Notwithstanding, this dependence is very weak and errors in T_e due to variations of the N_e are practically negligible. In our study we adopted an electron density of 300 cm^{-3} as a representative value. Electron densities in the range of 75 to 800 cm^{-3} have been measured in 30 Doradus (Feast 1961; Boeshaar et al. 1980). For densities in this range the errors in the electron temperature estimates would be below 0.2%.

4. Results and discussions

In Fig. 1 a sample of spectra from areas with different surface brightness is shown. The spatial profiles of the $\text{H}\beta$ flux, the $[\text{O III}](\lambda 4959 + \lambda 5007)/\lambda 4363$ ratio and the electron temperature are shown in Figs. 4–2. The position along the slit is positive to the west (PA = 90°) or northwest (PA = 26° and 58°) of the reference points whose equatorial coordinates are shown in Table 1. Table 2 presents some statistics of the data, including the number of different apertures, the median, the first and third quartiles (the limits between which 50% of the values lie), the minimum and maximum, and the mean, standard deviation and mean error weighted by the flux in $\text{H}\beta$.

The electron temperature estimates obtained are relatively homogeneous with fluctuations of very small amplitude along the three directions observed. For the entire set of 135 apertures observed, we found a weighted mean electron temperature of $10\,270 \pm 140$ (3σ) K. The temperature estimates present a small dispersion around the mean value of only 6%, measured as the weighted standard deviation. The individual mean temperatures for each of the three different slit positions are in agreement with the general average within an error of 3%.

No large-scale electron temperature gradient was found in 30 Doradus. Of course local observations, which are in fact integrations along the line of sight, tend to smooth out small spatial scale fluctuations of any line ratio. Nevertheless, point-to-point measurements are still able to detect global internal gradients. So, any significant large-scale systematic variation of the electron temperature should be revealed by our high signal-to-noise observations, as was the case of the studies of the planetary nebulae NGC 6720 (Garnett & Dinerstein 2001) and NGC 4361 (Liu 1998) and of the Orion Nebula (Walter et al. 1992).

As can be seen in Figs. 2–4, the areas with lower surface brightness in $\text{H}\beta$ tend to be associated with lower

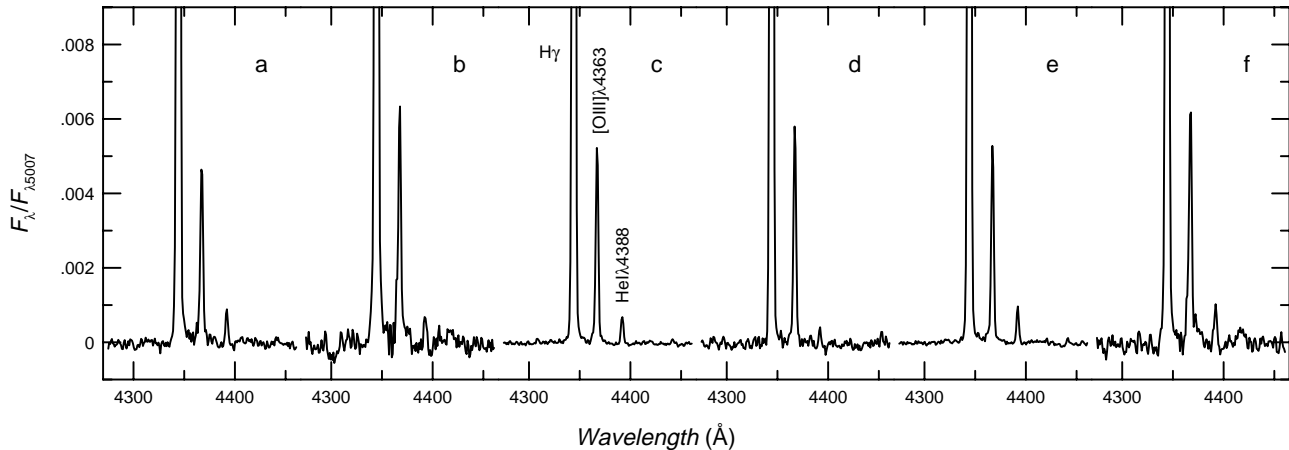


Fig. 1. A sample of spectra in the range of 4275 to 4460 Å from areas with different surface brightnesses along PA = 90°. The corresponding positions are marked in Fig. 2. To emphasize the variation of the [O III](λ4959 + λ5007)/λ4363 ratio, the flux scale was normalized to the peak of [O III]λ5007.

Table 2. [O III] ratio and electron temperature statistics.

	[O III](λ4959 + λ5007)/λ4363				T_e (K)			
	Position angle (°)				Position angle (°)			
	26	58	90	26+58+90	26	58	90	26+58+90
number of data	37	39	59	135	37	39	59	135
minimum	97 ± 14	115 ± 20	123 ± 9	97 ± 14	9766 ⁺¹⁴² ₋₁₃₁	9854 ⁺¹⁷¹ ₋₁₅₆	9707 ⁺¹⁰³ ₋₉₇	9707 ⁺¹⁰³ ₋₉₇
first quartile	125	141	190	155	10275	10195	9930	10003
median	156	173	203	190	10977	10598	10094	10296
third quartile	191	196	214	209	11838	11349	10291	10998
maximum	226 ± 11	219 ± 12	231 ± 8	231 ± 8	13011 ⁺⁸⁶⁹ ₋₆₆₆	12207 ⁺⁹⁰⁶ ₋₆₇₀	11918 ⁺³⁶⁸ ₋₃₂₁	13011 ⁺⁸⁶⁹ ₋₆₆₆
weighted mean	179	183	208	195	10598	10497	10015	10267
standard deviation	33.4	28.3	12.1	26.5	728	605	196	543

values for the [O III](λ4959 + λ5007)/λ4363 ratio and consequently with higher electron temperatures. If this apparent pattern is an artifact of the line flux estimation it will be certainly due to errors in the intensities of the [O III]λ4363 line since the other two lines are very strong and easily measured. In fact, Rola & Pelat (1994) have demonstrated that weak emission lines tend to be overestimated. To investigate this possibility we have recalculated the line intensities of [O III]λ4363 and Hγ with methods other than the initial one. Using the single line profile option of *splot* we have performed integrations by Gaussian fitting of each line individually with the central positions and line widths as free parameters and with an eye estimation of the continuum. With the deblending command of *splot* we have simultaneously fitted a linear function to the continuum in the range of 4275 to 4460 Å and Gaussian profiles with a single line width and free central wavelengths to the lines Hγ, [O III]λ4363 and the He Iλ4388. We have calculated the intensities for each spectrum individually and for their sums. We have also co-added each three contiguous apertures in order to increase the signal-to-noise. All these tests have confirmed the trend of lower temperatures at brighter spots, indicating that in the bright arcs of 30 Doradus, which correspond

to the densest areas, we find electron temperatures lower than in the most diffuse regions.

Interestingly, a similar anti-correlation between [O III] electron temperature and density can be seen in the data obtained for the Orion Nebula (Walter et al. 1992) and for the planetary nebula NGC 6720 (Garnett & Dinerstein 2001; Guerrero et al. 1997), the Orion Nebula presenting an outwards radial increase in temperature and decrease in density and NGC 6720 showing the opposite behaviour. These facts indicate that the density structure may play an important role in the production of the temperature fluctuations.

4.1. Comparison with other authors

We have recalculated the electron temperatures from measurements of the [O III] ratio found in the literature (Faulkner & Aller 1965; Peimbert & Torres-Peimbert 1974; Dufour et al. 1982; Mathis et al. 1985; Rosa & Mathis 1987) for 37 areas in 30 Doradus using the same atomic parameters and electron density adopted for our data. These estimates, with a mean value of 10 580 K and a standard deviation of 880 K, are in good agreement with those obtained from our own observations even for

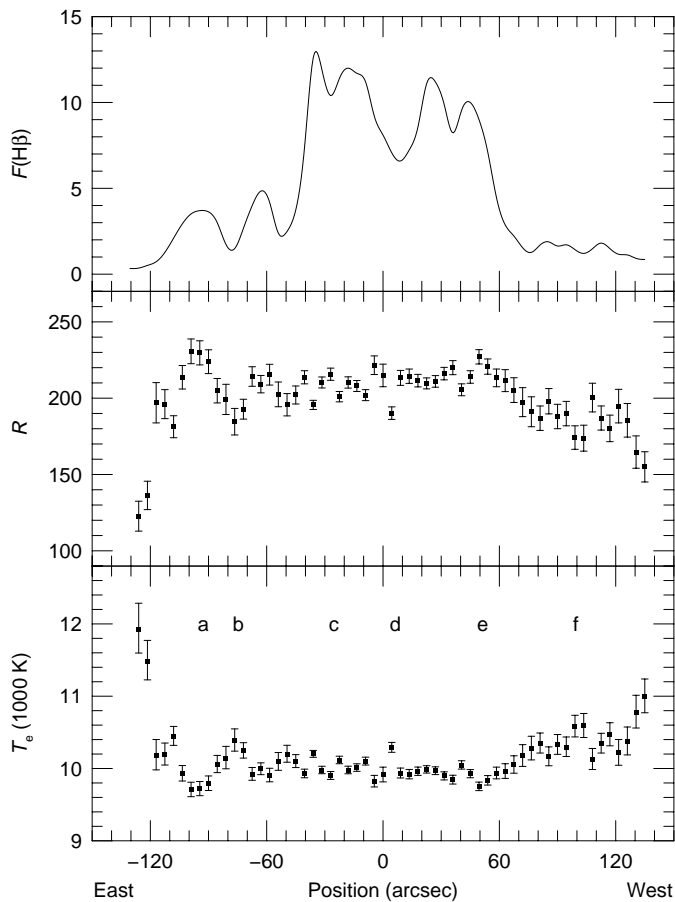


Fig. 2. Spatial profiles of the H β flux (in units of $10^{-13} \text{ ergs cm}^{-2} \text{ s}^{-1}$), the [O III]($\lambda 4959 + \lambda 5007$)/ $\lambda 4363$ ratio, R , and the electron temperature along PA = 90° . The labels indicate the positions corresponding to the spectra shown in Fig. 1.

regions not in common. In particular, the data from Rosa & Mathis (1987) obtained at 10 positions in the outer regions of 30 Doradus are entirely compatible with those from the core of the nebula which is another indication that the electron temperature in the O III ionization zone does not present striking large-scale spatial variations.

We have also compared our results with estimations of electron temperature based line-to-continuum ratios of radio recombination lines. Peck et al. (1997) have made interferometric observations of 30 Doradus in the H 90α , H 92α and H 109α lines smoothed to a resolution of $15'' \times 15''$. No significant temperature variations were found across the nebula. Although large differences between the optical and radio temperature estimates have been reported in the literature, the average global electron temperature of 9200 ± 1000 obtained from single dish observations of 30 Doradus (Shaver et al. 1983; Mezger et al. 1970; McGee et al. 1974) and from the data of Peck et al. (1997) integrated over the entire nebula is only 10% lower than our mean value. So, we verify that the mean optical and radio temperatures are consistent with each other within the error estimates. This is another indication that the fluctuations of electron temperature on a large spatial

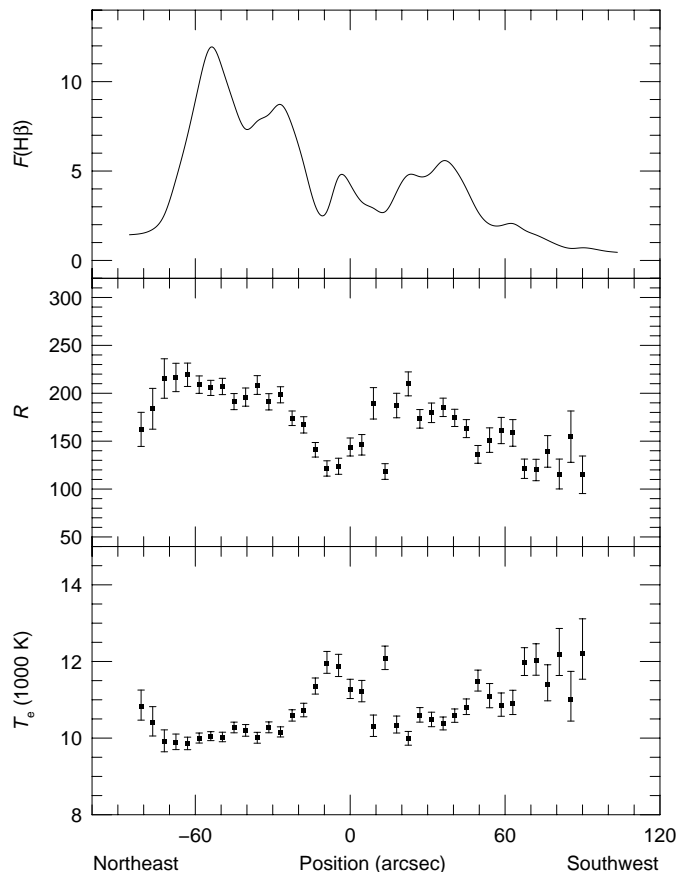


Fig. 3. Same as Fig. 2, but for PA = 58° .

scale are not strong in 30 Doradus since these two methods provide mean values of electron temperature with different weights for different regions, the collisionally excited lines being heavily weighted toward the hottest locations.

4.2. Magnitude of the electron temperature fluctuations

Following Peimbert (1967), the magnitude of the temperature fluctuations are usually quantified by the parameter t^2 defined as

$$t^2 = \frac{\int (T_e - T_0)^2 N_i N_e dV}{T_0^2 \int N_i N_e dV}, \quad (1)$$

with

$$T_0 = \frac{\int T_0 N_i N_e dV}{\int N_i N_e dV}, \quad (2)$$

where N_i is the density of the ion used to measure the temperature and the integrations are calculated over the observed volume V of the nebula. Essentially, T_0 and t^2 are the mean and the relative variance of the temperature distribution weighted by the square of the local density. Although t^2 cannot be directly measured, it can be estimated through the effects of the temperature fluctuations on the values of temperature or abundance obtained from different methods. By this method, values of

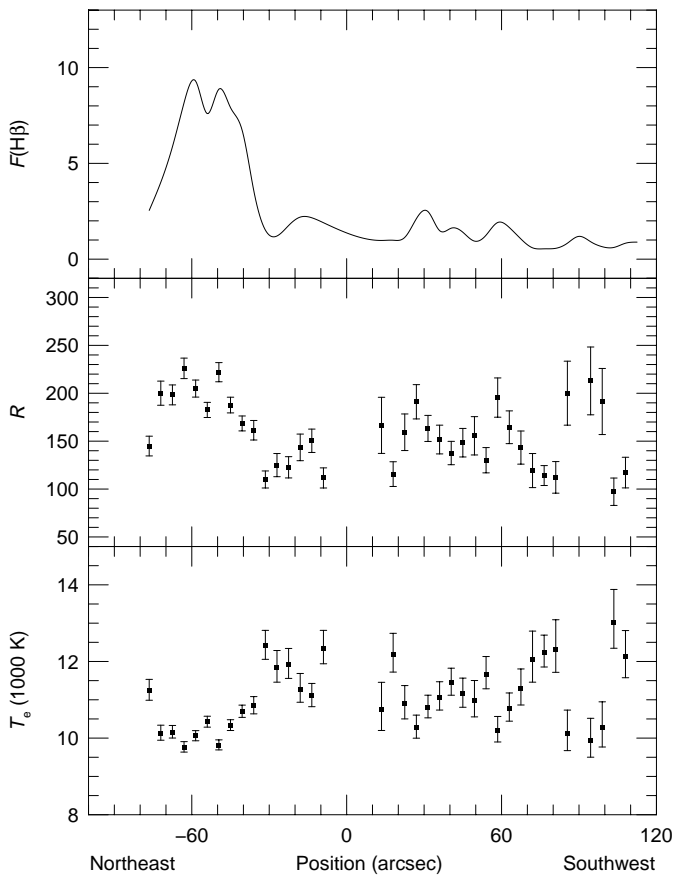


Fig. 4. Same as Fig. 2, but for PA = 26°.

$t^2 \approx 0.02$ – 0.10 have been attributed to planetary nebulae (Dinerstein et al. 1985; Liu & Danziger 1993; Peimbert et al. 1995), galactic (Esteban et al. 1998, 1999a,b) and extragalactic (Luridiana et al. 1999; Gonzalez-Delgado et al. 1994) H II regions. However, these high values for t^2 are not reproduced by the standard photoionization models, which predict $t^2 \leq 0.02$ (Gruenwald & Viegas 1995; Kingdon & Ferland 1995).

An independent estimation of t^2 can be obtained through point-to-point determinations of the electron temperature across the nebula. We may rewrite Eq. (1) and find a lower limit for t^2 as

$$t^2 = \frac{\int \langle (T_e - T_0)^2 \rangle_{\Omega} E_{\Omega} d\Omega}{T_0^2 \int E_{\Omega} d\Omega} \geq \frac{\int (\langle T_e \rangle_{\Omega} - T_0)^2 E_{\Omega} d\Omega}{T_0^2 \int E_{\Omega} d\Omega}, \quad (3)$$

where: $\langle \cdot \rangle_{\Omega}$ stands for the mean value weighted by the square density along the direction Ω ; $E_{\Omega} = \int N_i N_e dl$ is the emission measure; $d\Omega$ and dl are respectively the elements of solid angle and distance along the line of sight. A discrete approximation for the right hand side of expression 3 is given by (see Liu 1998)

$$t_s^2 = \frac{\sum_i (T_e^i - T_0)^2 F_i(\text{H}\beta)}{T_0^2 \sum_i F_i(\text{H}\beta)}, \quad (4)$$

where T_e^i and $F_i(\text{H}\beta)$ are the electron temperature and the H β flux obtained for the aperture i . Since part of the observed variance, $t_s^2(\text{obs})$, is due exclusively to errors in

the measurements, the final estimation of t_s^2 should be corrected by $t_s^2 = t_s^2(\text{obs}) - t_{\text{er}}^2$, t_{er}^2 being the relative mean quadratic error of the electron temperature measurements.

As the temperature measured at any point is a mean value along the line of sight, any small-scale temperature fluctuation would be smoothed out by the present observations. For this reason, it is clear that t_s^2 can only give a lower limit to t^2 . So, 2D mapping of the electron temperature in the nebula can possibly confirm the existence of large temperature fluctuations, but never disprove it. Theoretically, such small-scale temperature fluctuations are not expected and the temperature structure predicted follows a large-scale radial gradient. If indeed most of the temperature variation is along the radial direction, t_s^2 will be a bias but still useful estimator of t^2 . Liu (1998) has expected the difference between them to be smaller than a factor of 2. From the numerical simulations of point-to-point observations of Gruenwald & Viegas (1995), we have found that $0.1 \leq t_s^2/t^2 \leq 1$, with a median value of 0.7.

From our measurements of [O III] electron temperature in 135 areas of the 30 Doradus Nebula we have obtained a value of $t_s^2 = 0.0025$ for the variance of the projected temperature distribution, which corresponds to a dispersion amplitude of only 5%. A similar value of $t_s^2 = 0.002$ was found by Liu (1998) for the planetary nebula NGC 4361.

The small difference between the mean [O III] and radio electron temperatures also indicates a low amplitude for the temperature fluctuations in this nebula. From the expressions by Peimbert (1967) relating the [O III] and radio electron temperature estimates to T_0 and t^2 , we derive $t^2 = 0.02$, assuming the same values for T_0 and t^2 in the O⁺⁺ and H⁺ zones.

The low amplitude for the large-scale temperature fluctuations found in the 30 Doradus Nebula are consistent with the results of photoionisation models (Kingdon & Ferland 1995; Gruenwald & Viegas 1995) and are below the levels needed to explain the discrepancies between abundances derived from forbidden and recombination lines.

5. Conclusions

We present an observational study on the variation of the electron temperature in the 30 Doradus nebula based on long-slit spectrophotometry of high signal-to-noise ratio in the range of 4100 to 5030 Å. Electron temperatures were derived from the [O III]($\lambda 4959 + \lambda 5007$)/ $\lambda 4363$ ratios measured at 135 locations along three different directions. The main results are the following:

1. The electron temperature estimates obtained are fairly homogeneous. No large-scale electron temperature gradient has been detected in 30 Doradus. The compatibility between the present estimates with optical and radio temperature determinations found in the literature for other positions or for the entire nebula corroborates this conclusion.

2. An emission-weighted mean electron temperature of $10\,270 \pm 140$ (3σ) K was found.
3. Temperature fluctuations of small amplitude have been observed. The temperature distribution across the nebula presents a variance relative to the mean of $t_s^2 = 0.0025$ or equivalently a dispersion of only 5%. Temperature fluctuations of this magnitude are compatible with the prediction of photoionization models but are too small to be invoked as the cause of the discrepancy between the abundances derived from forbidden and recombination lines. However, we must emphasize that the existence of small-scale temperature fluctuations cannot be ruled out by the present observations.
4. The areas with lower surface brightness tend to present slightly higher electron temperatures. This would indicate that the bright arcs of 30 Doradus, which correspond to the densest regions, would have smaller electron temperatures than the most diffuse areas.

Acknowledgements. This work was partially supported by the Brazilian institutions CAPES, CNPQ and FAPERGS. We thank the anonymous referee for helpful comments and suggestions.

References

- Boeshaar, G. O., Boeshaar, P. C., Czyzak, S. J., Aller, L. H., & Lasker, B. M. 1980, *Ap&SS*, 68, 335
- Bowen, I. S. 1960, *ApJ*, 132, 1
- Dinerstein, H. L., Lester, D. F., & Werner, M. W. 1985, *ApJ*, 291, 561
- Dufour, R. J., Shields, G. A., & Talbot, R. J. 1982, *ApJ*, 252, 461
- Esteban, C., Peimbert, M., Torres-Peimbert, S., & Escalante, V. 1998, *MNRAS*, 295, 401
- Esteban, C., Peimbert, M., Torres-Peimbert, S., García-Rojas, J., & Rodríguez, M. 1999, *ApJS*, 120, 113
- Esteban, C., Peimbert, M., Torres-Peimbert, S., & García-Rojas, J. 1999, *Rev. Mex. Astron. Astrofis.*, 35, 65
- Faulkner, D. J., & Aller, L. H. 1965, *MNRAS*, 130, 393
- Feast, M. W. 1961, *MNRAS*, 122, 1
- García-Rojas, J., Esteban, C., Peimbert, M., & Torres-Peimbert, S. 1998, *Rev. Mex. Astron. Astrofis. Conf. Ser.*, 7, 176
- Garnett, D. R., & Dinerstein, H. L. 2001, *ApJ*, 558, 145
- Gonzalez-Delgado, R. M., et al. 1994, *ApJ*, 437, 239
- Gruenwald, R., & Viegas, S. M. 1992, *ApJ*, 78, 153
- Gruenwald, R., & Viegas, S. M. 1995, *A&A*, 303, 535
- Guerrero, M. A., Machado, A., & Chu, Y.-H. 1997, *ApJ*, 487, 328
- Howarth, I. D. 1983, *MNRAS*, 203, 301
- Hummer, D. G., & Storey, P. J. 1987, *MNRAS*, 224, 801
- Kingdon, J. B., & Ferland, G. J. 1995, *ApJ*, 450, 691
- Lennon, D. J., & Burke, V. M. 1994, *A&AS*, 103, 273
- Liu, X., & Danziger, J. 1993, *MNRAS*, 263, 256
- Liu, X.-W., Storey, P. J., Barlow, M. J., & Clegg, R. E. S. 1995, *MNRAS*, 272, 369
- Liu, X.-W. 1998, *MNRAS*, 295, 699
- Luridiana, V., Peimbert, M., & Leitherer, C. 1999, *ApJ*, 527, 110
- Mathis, J. S., Chu, Y.-H., & Peterson, D. E. 1985, *ApJ*, 292, 155
- McGee, R. X., Newton, L. M., & Brooks, J. W. 1974, *Aust. J. Phys.*, 27, 729
- Mezger, P. G., Wilson, T. L., Gardner, F. F., & Milne, D. K. 1970, *Astrophys. Lett.*, 5, 117
- Peck, A. B., Goss, W. M., Dickel, H. R., et al. 1997, *ApJ*, 486, 329
- Peimbert, M. 1967, *ApJ*, 150, 825
- Peimbert, M., & Torres-Peimbert, S. 1974, *ApJ*, 193, 327
- Peimbert, M., Torres-Peimbert, S., & Luridiana, V. 1995, *Rev. Mex. Astron. Astrofis.*, 31, 131
- Rola, C., & Pelat, D. 1994, *A&A*, 287, 676
- Rosa, M., & Mathis, J. S. 1987, *ApJ*, 317, 163
- Shaver, P. A., McGee, R. X., Newton, L. M., Danks, A. C., & Pottasch, S. R. 1983, *MNRAS*, 204, 53
- Walter, D. K., Dufour, R. J., & Hester, J. J. 1992, *ApJ*, 397, 196
- Wiese, W. L., Fuhr, J. R., & Deters, T. M. 1996, *JPCRD*, Monograph 7